

## Article

# Design and Evaluation of the Compact and Autonomous Energy Subsystem of a Wave Energy Converter

Marcin Drzewiecki <sup>1,2</sup>  and Jarosław Guziński <sup>1,\*</sup> 

<sup>1</sup> Department of Electric Drives and Energy Conversion, Faculty of Electrical and Control Engineering, Gdańsk University of Technology, Gabriela Narutowicza 11/12, 80-233 Gdańsk, Poland; marcin.drzewiecki@pg.edu.pl

<sup>2</sup> MpicoSys Embedded Pico Systems Sp. z o.o., Pomeranian Science and Technology Park, Al. Zwycięstwa 96/98, 81-451 Gdynia, Poland

\* Correspondence: jaroslaw.guzinski@pg.edu.pl; Tel.: +48-58-347-29-60

**Abstract:** This paper presents the results of the design process focused on the development of the energy subsystem (ES) of a wave energy converter (WEC). The ES is an important electrical part that significantly affects the energy reliability and energy efficiency of the entire WEC device. The designed ES was intended for compact WECs powering IoT network devices working in the distributed grid. The developed ES is an electronic circuit consisting of three cooperating subsystems used for energy conversion, energy storage, and energy management. The energy conversion subsystem was implemented as a set of single-phase bridge rectifiers. The energy storage subsystem was a battery-less implementation based on the capacitors. The energy management subsystem was implemented as a supervisory circuit and boost converter assembly. The designed ES was verified using the physical experiment method. The model experiment reflected the operation of the designed ES with a piezoelectric PZT-based WEC. The experimental results showed a 41.5% surplus of the energy supplied by ES over the energy demanded by the considered load at a duty cycle of ca. 6 min—37.2 mJ over 26.3 mJ, respectively. The obtained results have been evaluated and discussed. The results confirmed the designed ES as a convenient solution, which makes a significant contribution to the compact WECs that can be applied among others to a distributed grid of autonomous IoT network devices powered by free and renewable energy of sea waves. Finally, it will also enable sustainable development of mobile and wireless communication in those maritime areas where other forms of renewable energy may not be available.

**Keywords:** wave energy converters; WEC designs; renewable energy; onshore; nearshore; offshore; internet of things (IoT); hydropower; hydroelectric; energy saving



**Citation:** Drzewiecki, M.; Guziński, J. Design and Evaluation of the Compact and Autonomous Energy Subsystem of a Wave Energy Converter. *Energies* **2023**, *16*, 7699. <https://doi.org/10.3390/en16237699>

Academic Editors: Mário José Gonçalves Cavaco Mendes

Received: 13 October 2023

Revised: 12 November 2023

Accepted: 17 November 2023

Published: 21 November 2023



**Copyright:** © 2023 by the authors. Licensee MDPI, Basel, Switzerland. This article is an open access article distributed under the terms and conditions of the Creative Commons Attribution (CC BY) license (<https://creativecommons.org/licenses/by/4.0/>).

## 1. Introduction

The main motivation of the work presented in the paper was to contribute to the sustainable development of societies based on energy-neutral, power-reliable, compact, and autonomous wireless communication.

The first patent for a wave energy converter (WEC) was granted on 12 July 1799 [1,2]. That solution harvested the energy of the nearshore waves and converted it into the desired mechanical form. Since that time, many new patents and implementations of WECs have appeared both in model-scale laboratory conditions and in full-scale marine conditions: onshore, nearshore, and offshore [3]. This occurred especially in the era of electrical machines and advanced power electronics. The WECs implementations involving the electrical generators have emerged [4–9] and their development is still ongoing [10–12]. Simultaneously, a new approach involving the use of new materials to convert mechanical vibrations of water waves into electrical form began to arise [13–20]. Some of these solutions proved the advantage—in certain applications—of the maintenance-free piezoelectric materials (PMs) over the solutions involving the electromechanical machines operating as

generators. The authors of this article recognized, that the compact PM-based WEC may be a good response for the coming era of autonomous and distributed IoT devices [21–26] which have become more and more advanced [27–30], low-power [31–34], and common [35–38].

The above-mentioned PM implementations are promising; however, the dissipated energy harvested in this way needs to be properly processed and condensed in the energy storage and properly managed. The great works related to the use of new, maintenance-free materials [13–20] do not address yet the need for the development of electronic circuit of the energy subsystem (ES) ensuring appropriate processing and management of the stored energy.

The works described in this paper include the formulation of the use case scenario of the ES in Section 2. Section 3 presents the design of the ES which is an important part of the WEC, responsible for electrical energy conversion, storage, and management. The ES, its components and functions have been detailed and evaluated in this section. The proposed ES has been tailored to be as automated, autonomous, and compact as the above-mentioned IoT devices. These works addressed the need for the development of ES intended for IoT devices applied onshore, nearshore, and offshore, in situations where for environmental reasons other forms of renewable energy are—temporarily or permanently—not available. The experimental research has been detailed in Section 4. According to the results presented and discussed in Section 5, the main advantage of the designed ES is that it allows for the efficient use of the stored energy by deeply discharging the capacitors, even when their voltage is well below the needed supply voltage of the target load. The novelty of the presented works lies in providing the aimed solution: the convenient energy subsystem of the WEC converter, which combines the functions of energy converting, energy storage, and energy management. The benefits of the applied solution are concluded in Section 6.

## 2. Use Case Scenario: Autonomous and Distributed IoT Device

For the needs of evaluation of the designed ES, it was needed to establish the real-life use case scenario. Considering the practical application of ES to the piezoelectric PZT-based WEC, we derived the use case scenario. The scenario involved compact WEC with ES, applied to supply an autonomous IoT node. We considered the IoT node equipped with the 2.71" monochrome electronic paper display (e-paper) and low-power microcontroller supporting *LoRa* (LongRange) modulation. The 2.71" e-paper display is shown in Figure 1 [39].



**Figure 1.** The 2.71" monochrome e-paper display considered in the use case scenario—the actuator of the IoT node powered with the use of the designed ES. [39]

The production of these IoT nodes is commercially offered by MpicoSys, a company that provides complete solutions in the field of low-power technologies, especially using e-paper [40]. The considered IoT node can communicate over long distances in the order of kilometers. It can receive and display important messages regarding, e.g., air quality, water quality, weather alerts, security alerts, or weather forecasts. This IoT node and its energy

properties are described in detail in [39]. According to the experiment conducted there, the use case energy demand is 26.3 mJ per operating cycle. The operating cycle of the IoT node includes one communication cycle and refreshing the display content. The reliable power supply of such a node in conditions of wave energy harvesting requires the use of a converter with a tailored ES.

### 3. Energy Subsystem

One of the crucial elements of a compact and autonomous WEC is the ES. The design of the ES has been tailored to the intended use case of the compact WEC powering the IoT network devices working in the distributed grid. The design of the ES and its topology are described as follows and afterward evaluated in the context of the use case scenario. The considered ES of the WEC consisted of

- an energy conversion module,
- an energy storage module,
- an energy management module.

The energy conversion module was intended to convert the energy of high-voltage peaks at the output of the PM-based converter. This module converted the alternating voltage into the form of positive pulsating voltage, convenient for storing and further processing. The energy conversion module consisted of two *B04BF* single-phase bridge rectifiers. The *B04BF* rectifiers were chosen due to their low forward voltage drop, low leakage current, and high forward surge capability. The set of two rectifiers has been applied as the considered WEC PZT transducer was a double side covered with PM.

The energy storage module was intended to collect energy so that it was available in a convenient form when needed. As the ES was designed to be sustainable, it needed to be applied as battery-free. The battery-free and maintenance-free approach implied that the energy storage module consisted of six *TAJE108K004RNJ* tantalum capacitors dedicated to general low-power DC/DC and low dropout (LDO) applications. The *TAJE108K004RNJ* tantalum capacitors were chosen due to their long lifespan, long-term stability, and superior frequency characteristics suitable for positive pulsating voltage peaks on the output of the energy conversion module.

The energy management module was intended to ensure the efficiency of energy harvesting, storage, and consumption. It consisted of:

- *MAX824LEUK+T* supervisory circuit with reset output;
- *MCP1624-I/MC* low-voltage input boost regulator with an application;
- circuit passive components: MLCC capacitors, resistors, and inductor listed in items 8–13 in Table 1;
- *MCP1703-3302E/DB* low quiescent current LDO regulator;
- *DMG1013T-7* P-channel enhancement mode MOSFET transistor;
- *SS14* Schottky barrier rectifier diodes.

The *MAX824LEUK+T* was chosen due to its very low supply current of 10  $\mu$ A and sufficient output current of 20 mA. The *MCP1624-I/MC* was chosen due to its low quiescent current, low start-up voltage, and low operating input voltage suitable for sucking energy from the capacitors as their voltage decreases as the energy stored in them is consumed. The *MCP1703-3302E/DB* was chosen due to its low dropout voltage. The *DMG1013T-7* was applied because it is dedicated to the power management functions and due to its low on-resistance, low input capacitance, fast switching speed, and low input and output leakages. The *SS14* was chosen due to its low leakage current.

The ES circuit has been designed to perform the operation as follows. The *TAJE108K004RNJ* energy storage capacitors are charged with energy from the PM-based WEC via *B04BF* rectifiers. The positive leads of the *TAJE108K004RNJ* energy storage capacitors were connected via the first *SS14* Schottky diode to the voltage monitoring pin of the *MAX824LEUK+T* supervisory circuit. The supervisory circuit monitors the voltage level on the *TAJE108K004RNJ* energy storage capacitors. The volt-

age level corresponds to the energy harvested in the capacitors. When the appropriate amount of energy is accumulated and the capacitor's voltage reaches the threshold value, then the *RESET* output of *MAX824LEUK+T* drives the *DMG1013T-7* transistor gate to turn on the transistor. Turning on the transistor supplies power to the *MCP1624-I/MC* boost regulator from the capacitors. Subsequently, the boosted voltage is stepped down using the *MCP1703-3302E/DB* LDO regulator. The voltage level on the output of the LDO regulator is appropriate to supply most microcontrollers such as those used in IoT devices. At the same time, the boosted voltage on the output of the boost regulator is applied via the second *SS14* Schottky diode to the voltage monitoring pin of the *MAX824LEUK+T* supervisory circuit. The applied *SS14* diodes enable appropriate processing of voltage signals to ensure proper operation of the energy management module. The boosted level on the voltage monitoring pin holds the low level on the *RESET* pin. Consequently, the transistor remains turned on even if the voltage of capacitors decreases below the threshold as the energy stored in them is consumed. This allows us to keep sucking the energy from the capacitors and boosting their voltage to supply the load—the IoT device—with the appropriate voltage for the time it takes to complete the duty cycle. The supervisory circuit will turn off the transistor only when the energy stored in the capacitors drops so much that their voltage is below the operating input voltage of the boost regulator. Then the next switching on will only take place when the capacitor's voltage reaches the threshold value again. The schematic diagram of the ES circuit is presented in Figure 2.

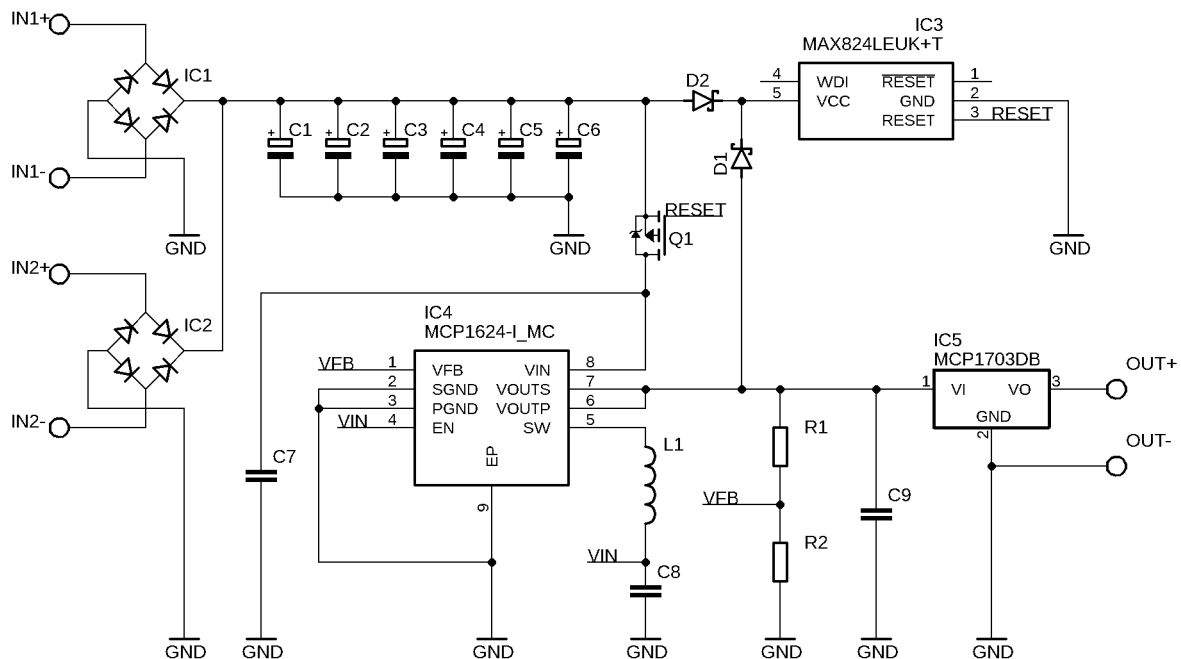


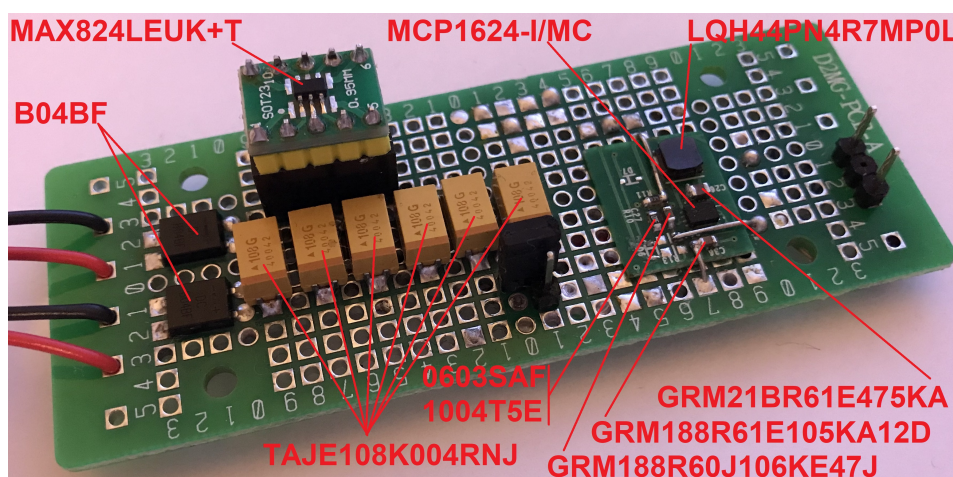
**Figure 2.** Schematic diagram of the designed energy subsystem circuit consisted of the energy conversion module, energy storage module, and energy management module.

The electronic components applied to the ES circuit are listed in Table 1.

The implementation of the designed ES is presented in Figure 3. The schematic diagram was implemented on a prototype D2MG-PCB-A universal board with a width of 32.8 mm, a length of 86.9 mm, and a thickness of 1.6 mm.

**Table 1.** List of electronic components applied to the energy subsystem.

Item	Reference	Description	Value	Part Number	Quantity
1	IC1, IC2	Bridge rectifier	–	<i>B04BF</i>	2
2	IC3	Supervisory circuit	4.63 V	<i>MAX824LEUK+T</i>	1
3	IC4	Boost regulator	–	<i>MCP1624-I/MC</i>	1
4	IC5	LDO regulator	3.3 V	<i>MCP1703-3302E/DB</i>	1
5	Q1	P-MOSFET transistor	–	<i>DMG1013T-7</i>	1
6	D1, D2	Schottky diode	–	<i>SS14</i>	2
7	C1...C6	Tantalum capacitor	1 mF	<i>TAJE108K004RNJ</i>	6
8	C7	MLCC capacitor	4.7 $\mu$ F	<i>GRM21BR61E475KA</i>	1
9	C8	MLCC capacitor	1 $\mu$ F	<i>GRM188R61E105KA12D</i>	1
10	C9	MLCC capacitor	10 $\mu$ F	<i>GRM188R60J106KE47J</i>	1
11	R1	Resistor	1 M $\Omega$	<i>0603SAF1004T5E</i>	1
12	R2	Resistor	330 k $\Omega$	<i>CRCW0402330KFKED</i>	1
13	L1	Inductor	4.7 $\mu$ H	<i>LQH44PN4R7MP0L</i>	1

**Figure 3.** The implementation of the designed energy subsystem.

#### 4. Experimental Research

The research was carried out using a physical experiment on a model. For the purposes of the experiment, a PZT transducer was connected to the input of the ES to model the WEC operation. The transducer applied to the experiment was a bimorph piezoelectric ceramic transducer made of brass and a double side covered with a PZT material. One side was connected to the *IN1* input terminals and the other side to the *IN2* input terminals. The PZT material corresponded to the ones applied in PM-based WECs described in the related works [17,41]. The bimorph piezoelectric ceramic transducer is shown in Figure 4. The transducer's brass material had a width of 33 mm and a length of 80 mm. The transducer's double side PZT material had a width of 30 mm and a length of 60 mm. The transducer's overall thickness was 0.6 mm. The operation of the transducer under the influence of a force at a frequency of 1 Hz has been performed. The force was applied to the center of the transducer plane and was longitudinally deforming it. At this time, the transducer's long ends were fixed to a stationary support. The applied force resulted in deformation with an amplitude of 3 mm. This corresponded to 6 mm peak-to-peak deformation. This resulted in the generation of voltage at the ES input terminals and the operation of the energy conversion, energy storage, and energy management ES modules.

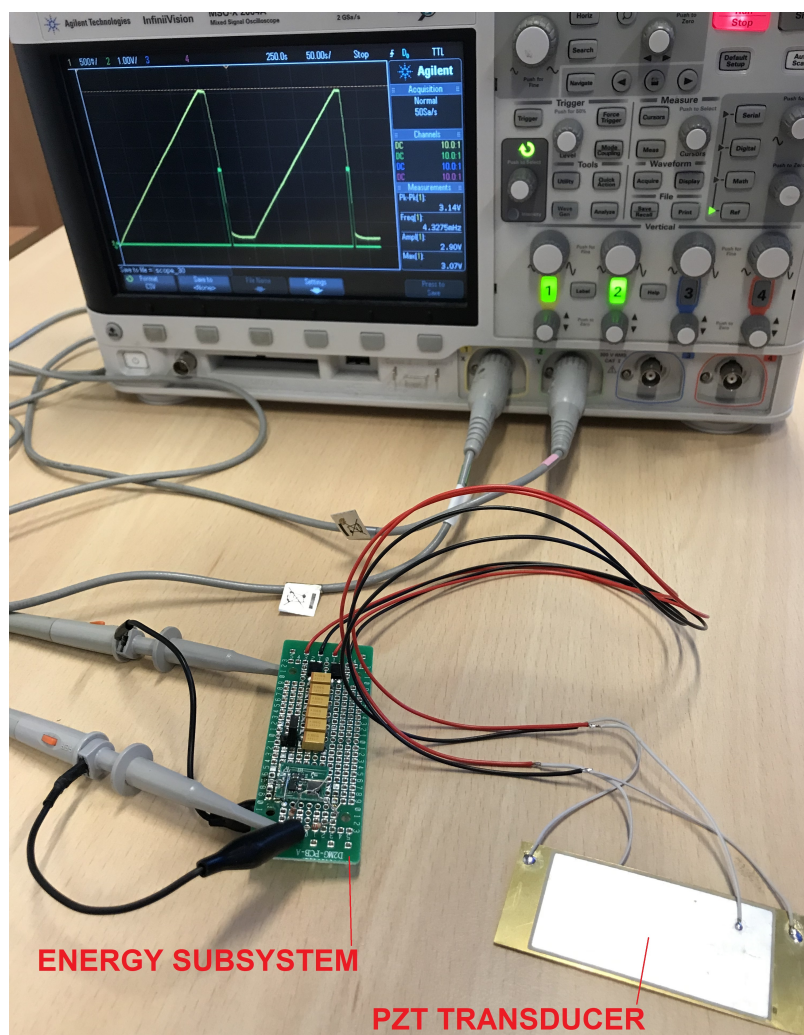


**Figure 4.** The experimental measurement setup: bimorph piezoelectric ceramic transducer connected to the energy subsystem.

The ES load was modeled by connecting a 2 k $\Omega$  resistance to the ES *OUT* terminals. The  $V_{CAP}$  voltage harvested in the energy storage module and the  $V_{OUT}$  voltage supplied to the ES load have been measured with the use of *AGILENT TECHNOLOGIES DSO-X 2004A* oscilloscope. The oscilloscope measurement probes were connected to the leads of the tantalum capacitors  $C1 \dots C6$  and to ES's *OUT* output terminals. The applied  $R_L$  load resistance was known. The designed and applied  $C_{ES}$  energy storage capacitance was equal to 6 mF. Based on the measured voltages, known parameters, and physical relationships, the corresponding amounts of energy could be calculated. The amount of the  $E_H$  energy harvested in the energy storage module is given by Formula (1) [42].

$$E_H = \frac{1}{2} C_L V_{CAP}^2. \quad (1)$$

The  $E_L$  energy consumed in time period  $T$  by the load can be calculated as (2) [43].

$$E_L = \frac{V_{OUT}^2}{R_L} T. \quad (2)$$

The energy analysis results obtained in this way were the basis for further evaluation of the designed ES. The experimental measurement setup is shown in Figure 4.

## 5. Results

The physical experiment and measurement setup have been detailed in the previous section. According to the measurements performed during the ES operation, energy was successfully harvested and the  $V_{CAP}$  voltage on the leads of the energy storage module rose from 0 V to 4.74 V in 348 s. After collecting the amount of energy, at which the  $V_{CAP}$  voltage exceeded the reset threshold, the energy management system turned on the power supply to the load in 348 s. Then, the  $V_{OUT}$  supply voltage was applied to the output of the ES, and the load was supplied with an average voltage of 3.2 V for 7 s. The power management module worked properly and kept the load supplied with an average voltage of 3.2 V even when the energy storage module voltage dropped to 1.25 V. The recorded voltage waveforms are presented in Figure 5.

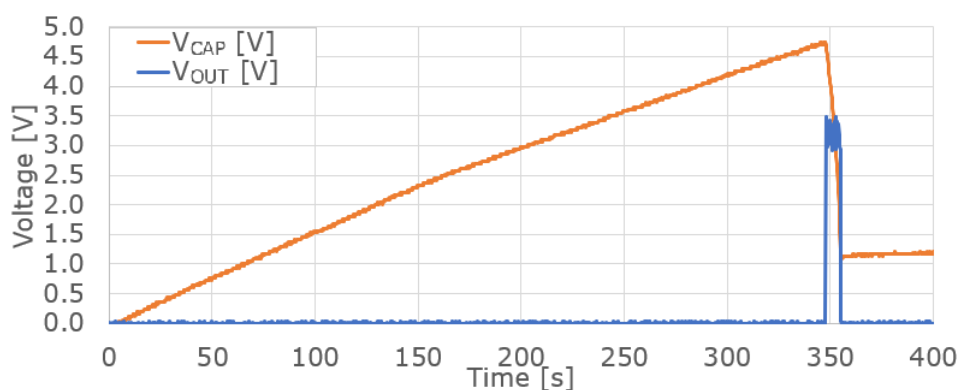


**Figure 5.** The voltages measured during the operation of the ES— $V_{CAP}$  on its input terminals and  $V_{OUT}$  on its output terminals.

During the energy harvesting process and increasing the  $V_{CAP}$  voltage, the energy rose from 0 mJ to 67.5 mJ in 348 s. Then, the load was supplied and 63.4 mJ of energy was consumed by ES to power the load, with 4.1 mJ of unused residual energy remaining in the energy storage. The calculated energy waveform is presented in Figure 6.

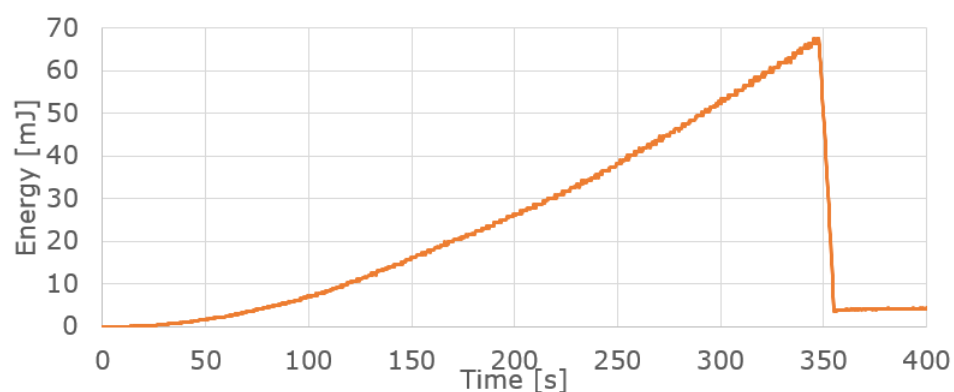


**Figure 6.** The energy stored during the operation of the ES increases while harvesting and decreases when powering the load, and the residual energy remains.

The  $V_{OUT}$  supply voltage applied to the load is shown in Figure 7. When the required amount of energy was collected, so the  $V_{CAP}$  voltage exceeded the reset threshold, the energy management system turned on the  $V_{OUT}$  voltage supply to the load. An average voltage of 3.2 V at a load of 1.6 mA was applied for 7 s. This period of time is sufficient for the communication and actuation cycle of many IoT devices, as well as for the autonomous and distributed IoT devices considered in the use case scenario of the current paper.

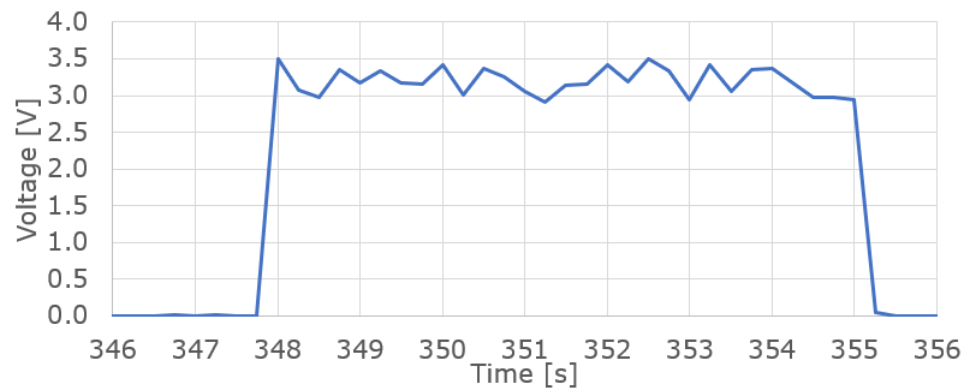


**Figure 7.** The  $V_{OUT}$  supply voltage measured during the operation of the ES.

As we knew the  $V_{OUT}$  voltage and  $R_L$  resistance, we could calculate the load current based on Ohm's law. Such calculated load current is shown in Figure 8. When the average  $V_{OUT}$  voltage of 3.2 V is applied to the load resistance of 2 k $\Omega$ , then the average load current of 1.6 mA flows for 7 s. After this time, the energy from the energy storage is consumed to the level at which the power supply is cut off.

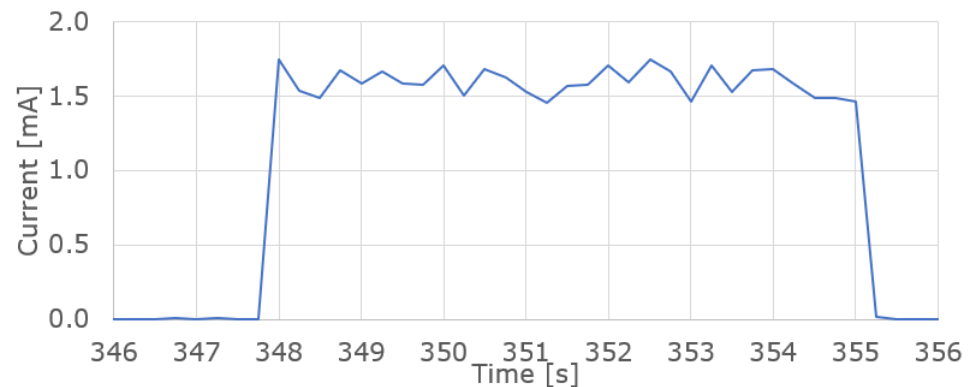


**Figure 8.** The load current during operation of the ES.

Based on the load voltage and load current, we could calculate the load power shown in Figure 9. When the average  $V_{OUT}$  voltage of 3.2 V is applied to the load and the average load current of 1.6 mA flows, then the load is powered by 5.1 mW for 7 s. Such power and time are efficient for the IoT device considered in the use case scenario of the ES.

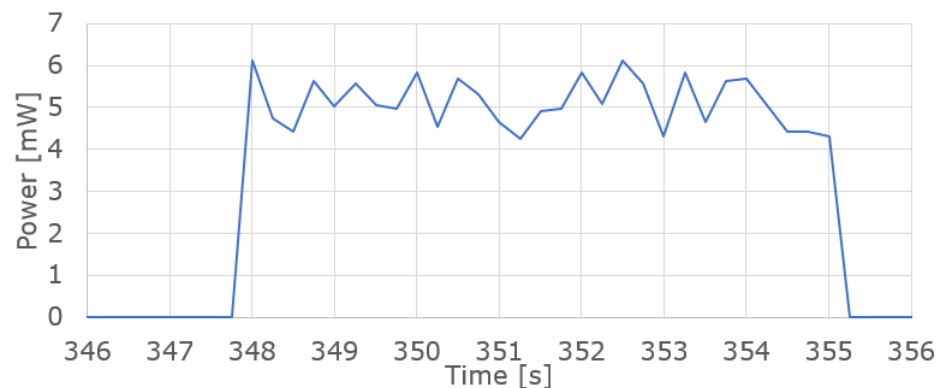


**Figure 9.** The load power during operation of the ES.

Based on Formula (2), we could calculate the  $E_{OUT}$  energy supplied to the load during one operation cycle of the ES. The amount of the supplied  $E_{OUT}$  is equal to 37.2 mJ, as shown in Figure 10.



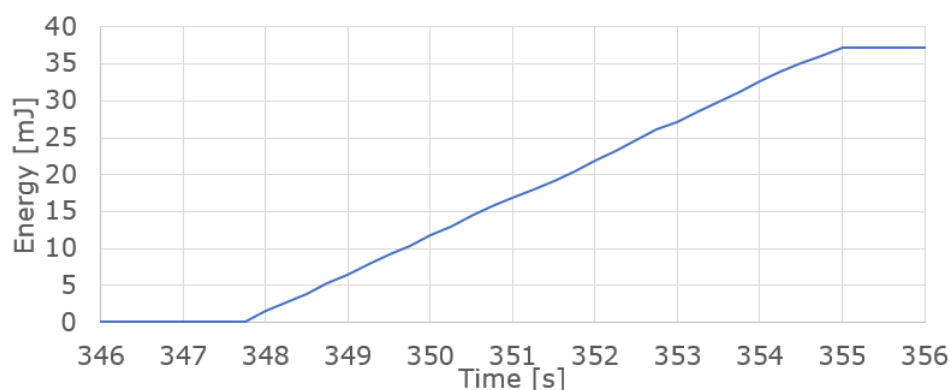


**Figure 10.** The energy supplied to the load during operation of the ES.

A summary of the ES's energy performance versus the use case scenario energy demand is presented in Table 2.

**Table 2.** Summary of WEC energy conversion performance under the load and the modeled impact of the considered wave.

Parameter	Value	Unit
ES energy harvested	67.5	mJ
ES energy delivered	37.2	mJ
ES efficiency	55.1	%
ES unused residual energy	4.1	mJ
ES energy utilization rate	93.9	%
Use case energy demand	26.3	mJ
ES energy surplus over demand	10.9	mJ
ES relative energy surplus	41.5	%

In accordance with the results of the measurements, the energy supplied to the load from ES was equal to 37.2 mJ. The amount of energy demanded for the considered use case was equal to 26.3 mJ. Both energy scores correspond to a duty cycle of less than 6 min. The experiment results confirmed that the designed ES enables the autonomous operation of the IoT device. The designed ES ensures convenient energy management, which allows for in-depth consumption of the stored energy. This ensures a high, 93.9% energy utilization rate. However, future work should consider an improvement of the 55.1% ES efficiency. Such efficiency results from losses occurring during the energy conversion. There are losses in the circuits of the boost regulator *MCP1624 – I/MC*. The load current is relatively small which reduces the efficiency. The difference in input and output voltages becomes more and more significant as the energy storage discharges, then the boost action becomes more lossy. The applied inductor *LQH44PN4R7MP0L* has existing and inevitable Equivalent Series Resistance (ESR). These factors make the boost conversion take place with a certain efficiency. There are also losses in the *MCP1703 – 3302E/DB* LDO regulator. Both of these series-connected ICs and their peripheral circuits convert energy with the efficiency rate, which for the current configuration is 55.1%

The results obtained from the current indoor experiment were compared with those obtained from another experiment conducted in the water waves environment for better evaluation. The results of the related works and experiments on the EPAM-based WEC detailed in [13] were used for this purpose. The electrical energy generated there under the impact of the water wave force at the frequency equal to 1 Hz and for different wave heights (HW), for each cycle of the wave was: 7.3 mJ at HW of 2.0 cm; 15.8 mJ at HW of 3.0 cm; 23.5 mJ at HW of 4.0 cm; 26.4 mJ at HW of 6.0 cm. Such a yield exceeds that of PZT-based WEC in the current study. However, the EPAM-based solution requires an external high-voltage source due to the operating principle of the EPAM material [13]. This requirement disqualifies the EPAM-based converter from being compact and autonomous.



Simultaneously, the currently considered PZT-based solution provides the desired amount of energy. Therefore, the current solution has been evaluated as more applicable to compact, autonomous, and sustainable IoT devices.

## 6. Conclusions

The results of the research meet the anticipations. The application of the designed ES to the compact PZT-based WEC will enable the realization of the intended use case, ensuring the energy surplus. The designed and applied ES has been experimentally validated as capable of powering the distributed and autonomous IoT device. Moreover, the ES enables the energy harvested in the battery-less energy storage to be consumed more completely. The energy management module of the ES maintains the correct load supply voltage level even when the storage voltage drops significantly. The designed ES contributes to the development of compact WECs, especially those applied to a distributed grid of autonomous IoT network devices powered by the energy of sea waves. Further application of this solution to the compact WECs will support the sustainable development of mobile and wireless communication in those maritime areas where other forms of renewable energy may not be available—e.g., lack of sunlight for PV panels at night. One of the greatest advantages of the developed solution is its scalability. It is both quantitatively scalable for a larger number of IoT nodes in distributed networks and also scalable in terms of size for larger facilities, e.g., large coastal wave breakers converting the energy of waves crashing on the shores.

As the future scope of the research, it is needed to improve the ES efficiency of 55.1%. This would allow for the use of smaller energy storage and reduce the future costs of each electronic ES intended for compact WECs. The present study is limited to indoor experiments and evaluation of the energy subsystem, that harvests energy from the mechanically oscillated PZT transducer and supplies the model of load. In future research, we intend to develop the optimized hydromechanical part of the compact WEC to combine the electronic and hydromechanical parts and test them in real environments in water waves. In further research, we also intend to validate the ES with an operating IoT node device communicating with the network. Future works planned in this way will help overcome current limitations.

**Author Contributions:** Conceptualization, M.D. and J.G.; methodology, M.D. and J.G.; software, M.D.; validation, M.D. and J.G.; formal analysis, M.D.; investigation, M.D.; resources, M.D.; data curation, M.D.; writing—original draft preparation, M.D. and J.G.; writing—review and editing, J.G.; visualization, M.D.; supervision, J.G.; project administration, M.D. and J.G.; funding acquisition, M.D. and J.G. All authors have read and agreed to the published version of the manuscript.

**Funding:** The APC was funded by the Faculty of Electrical and Control Engineering at the Gdańsk University of Technology.

**Data Availability Statement:** The data presented in this study are available on request from the M.D. author.

**Conflicts of Interest:** The authors that are working at MpicoSys Embedded Pico Systems Sp. z o.o., declare no conflict of interest.

## Abbreviations

The following abbreviations are used in this manuscript:

APC	Article processing charges
DC	Direct current
EPD	Electronic paper display
ES	Energy subsystem
IoT	Internet of Things
LDO	Low dropout



MOSFET	Metal-oxide-semiconductor field-effect transistor
PEC	Prototype power electronic circuit
PM	Piezoelectric material
PZT	Lead zirconate titanate
WEC	Wave energy converter

## References

- Girard, P.; Girard, S. Brevet D'invention de Quinze ans, Pour Divers Moyens d'Employer les Vagues de la Mer, Comme Moteurs. Available online: [https://www.labima.unifi.it/upload/sub/seminars/Florence%20Slides%202\\_PhD.pdf](https://www.labima.unifi.it/upload/sub/seminars/Florence%20Slides%202_PhD.pdf) (accessed on 16 November 2023).
- Titah-Benbouzid, H.; Benbouzid, M. Ocean wave energy extraction: Up-to-date technologies review and evaluation. In Proceedings of the 2014 International Power Electronics and Application Conference and Exposition, Shanghai, China, 5–8 November 2014; pp. 338–342. [\[CrossRef\]](#)
- Clément, A.; McCullen, P.; Falcão, A.; Fiorentino, A.; Gardner, F.; Hammarlund, K.; Lemonis, G.; Lewis, T.; Nielsen, K.; Petroncini, S.; et al. Wave energy in Europe: Current status and perspectives. *Renew. Sustain. Energy Rev.* **2002**, *6*, 405–431. [\[CrossRef\]](#)
- Yemm, R. *The History and Status of the Pelamis Wave Energy Converter*; IMECHE Seminar: London, UK, 1999.
- Heath, T.; Whittaker, T.J.T.; Boake, C.B. The design, construction and operation of the LIMPET wave energy converter (Islay Scotland). In Proceedings of the 4th EWEC, Aalborg, Denmark, 4–6 December 2000.
- Falcao, A.F.d.O. *Design and Construction of the OWC Wave Power Plant at the Azores*; IMECHE Seminar: London, UK, 1999.
- Sørensen, H.C.; Hansen, R.; Friis-Madsen, E.; Panhauser, W.; Mackie, G.; Hansen, H.H.; Frigaard, P.; Hald, T.; Knapp, W.; Keller, J.; et al. The Wave Dragon—Now ready for Test in real sea. In Proceedings of the 4th EWEC, Aalborg, Denmark, 4–6 December 2000.
- Rademakers, L.W.M.M.; van Schie, R.G.; Schutte, R.; Vriesema, B.; Gardner, F. Physical model testing for characterizing the AWS. In Proceedings of the 3rd EWEC, Patras, Greece, 30 September–2 October 1998.
- Lagoun, M.S.; Benalia, A.; Benbouzid, M.E.H. Ocean wave converters: State of the art and current status. In Proceedings of the 2010 IEEE Energycon, Manama, Bahrain, 18–22 December 2010; pp. 636–642.
- Jusoh, M.A.; Ibrahim, M.Z.; Daud, M.Z.; Albani, A.; Mohd Yusop, Z. Hydraulic Power Take-Off Concepts for Wave Energy Con-version System: A Review. *Energies* **2019**, *12*, 4510. [\[CrossRef\]](#)
- Zapata, H.M.; Perez, M.A.; Marquez Alcaide, A. Control of Cascaded Multilevel Converter for Wave Energy Applications. *Energies* **2023**, *16*, 71. [\[CrossRef\]](#)
- Wang, Z.; Wu, S.; Lu, K.-H. Improvement of Stability in an Oscillating Water Column Wave Energy Using an Adaptive Intelligent Controller. *Energies* **2023**, *16*, 133. [\[CrossRef\]](#)
- Chiba, S.; Waki, M.; Wada, T.; Hirakawa, Y.; Masuda, K.; Ikoma, T. Consistent ocean wave energy harvesting using electroactive polymer (dielectric elastomer) artificial muscle generators. *Appl. Energy* **2013**, *104*, 497–502. [\[CrossRef\]](#)
- Chou, X.; Zhu, J.; Qian, S.; Niu, X.; Qian, J.; Hou, X.; Mu, J.; Geng, W.; Cho, J.; He, J.; et al. All-in-one filler-elastomer-based high-performance stretchable piezoelectric nanogenerator for kinetic energy harvesting and self-powered motion monitoring. *Nano Energy* **2018**, *53*, 550–558. [\[CrossRef\]](#)
- Mathew, A.T.; Liu, C.; Ng, T.Y.N.; Koh, S.J.A. A high energy dielectric-elastomer-amplified piezoelectric (DEAMP) to harvest low frequency motions. *Sens. Actuators A Phys.* **2019**, *294*, 61–72. [\[CrossRef\]](#)
- Mutsuda, H.; Tanaka, Y.; Doi, Y.; Moriyama, Y. Application of a flexible device coating with piezoelectric paint for harvesting wave energy. *Ocean Eng.* **2019**, *172*, 170–182. [\[CrossRef\]](#)
- Nabavi, S.F.; Farshidianfar, A.; Afsharfard, A.; Khodaparast, H.H. An ocean wave-based piezoelectric energy harvesting system using breaking wave force. *Int. J. Mech. Sci.* **2019**, *151*, 498–507. [\[CrossRef\]](#)
- Chiba, S.; Waki, M. Innovative power generator using dielectric elastomers (creating the foundations of an environmentally sus-tainable society). *Sustain. Chem. Pharm.* **2020**, *15*, 100205. [\[CrossRef\]](#)
- Li, X.; Xiao, Q. A Numerical Study on an Oscillating Water Column Wave Energy Converter with Hyper-Elastic Material. *Energies* **2022**, *15*, 8345. [\[CrossRef\]](#)
- Wang, C.; Luo, Z.; Lu, Z.; Shang, J.; Wang, M.; Zhu, Y. Design and CFD Analysis of the Energy Efficiency of a Point Wave Energy Converter Using Passive Morphing Blades. *Energies* **2023**, *16*, 204. [\[CrossRef\]](#)
- Weiser, M. The Computer for the 21st Century. *Sci. Am.* **1991**, *265*, 94–104. [\[CrossRef\]](#)
- Raji, R.S. Smart networks for control. *IEEE Spectr.* **1994**, *31*, 49–55. [\[CrossRef\]](#)
- Qiu, R.; Zhang, Z. Design of enterprise Web servers in support of instant information retrievals. *IEEE RFID Virtual J.* **2003**. [\[CrossRef\]](#)
- Rammig, F.J.; Gotz, M.; Heimfarth, T.; Janacik, P.; Oberthur, S. Real-time Operating Systems for Self-coordinating Embedded Sys-tems. In Proceedings of the Ninth IEEE International Symposium on Object and Component-Oriented Real-Time Distributed Computing (ISORC'06), Gyeongju, Republic of Korea, 24–26 April 2006. [\[CrossRef\]](#)
- Dolin, R.A. Deploying the “Internet of things”. In Proceedings of the International Symposium on Applications and the Internet (SAINT'06), Phoenix, AZ, USA, 23–27 January 2006. [\[CrossRef\]](#)

26. Mattern, F.; Floerkemeier, C.: Vom Internet der Computer zum Internet der Dinge. *Informatik-Spektrum* **2010**, *33*, 107–121. [[CrossRef](#)]
27. Miraz, M.H.; Ali, M.; Excell, P.S.; Picking, R. A review on Internet of Things (IoT), Internet of Everything (IoE) and Internet of Nano Things (IoNT). In Proceedings of the 2015 Internet Technologies and Applications (ITA), Wrexham, UK, 8–11 September 2015; pp. 219–224. [[CrossRef](#)]
28. Elhoseny, M.; Haseeb, K.; Shah, A.A.; Ahmad, I.; Jan, Z.; Alghamdi, M.I. IoT Solution for AI-Enabled PRIVACY-PREServing with Big Data Transferring: An Application for Healthcare Using Blockchain. *Energies* **2021**, *14*, 5364. [[CrossRef](#)]
29. Nandi, S.; Mishra, M.; Majumder, S. *Usage of AI and Wearable IoT Devices for Healthcare Data: A Study*; IEEE: Piscataway, NJ, USA, 2023; pp. 315–337. [[CrossRef](#)]
30. Lai, Q.H.; Lai, C.S.; Lai, L.L. *Smart Health Based on Internet of Things (IoT) and Smart Devices*; IEEE: Piscataway, NJ, USA, 2023; pp. 425–462. [[CrossRef](#)]
31. Hiramoto, T.; Takeuchi, K.; Mizutani, T.; Ueda, A.; Saraya, T.; Kobayashi, M.; Yamamoto, Y.; Makiyama, H.; Yamashita, T.; Oda, H.; et al. Ultra-low power and ultra-low voltage devices and circuits for IoT applications. In Proceedings of the 2016 IEEE Silicon Nanoelectronics Workshop (SNW), Honolulu, HI, USA, 12–13 June 2016; pp. 146–147. [[CrossRef](#)]
32. Frøytlog, A.; Cenkeramaddi, L.R. Design and Implementation of an Ultra-Low Power Wake-up Radio for Wireless IoT Devices. In Proceedings of the 2018 IEEE International Conference on Advanced Networks and Telecommunications Systems (ANTS), Indore, India, 16–19 December 2018; pp. 1–4. [[CrossRef](#)]
33. Frøytlog, A.; Haglund, M.A.; Cenkeramaddi, L.R.; Jordbru, T.; Kjellby, R.A.; Beferull-Lozano, B. Design and implementation of a long-range low-power wake-up radio for IoT devices. In Proceedings of the 2019 IEEE 5th World Forum on Internet of Things (WF-IoT), Limerick, Ireland, 15–18 April 2019; pp. 247–250. [[CrossRef](#)]
34. Ciccina, S.; Giordanengo, G.; Vecchi, G. Energy Efficiency in IoT Networks: Integration of Reconfigurable Antennas in Ultra Low-Power Radio Platforms Based on System-on-Chip. *IEEE Internet Things J.* **2019**, *6*, 6800–6810. [[CrossRef](#)]
35. Vishwakarma, S.K.; Upadhyaya, P.; Kumari, B.; Mishra, A.K. Smart Energy Efficient Home Automation System Using IoT. In Proceedings of the 2019 4th International Conference on Internet of Things: Smart Innovation and Usages (IoT-SIU), Ghaziabad, India, 18–19 April 2019; pp. 1–4. [[CrossRef](#)]
36. Agarwal, K.; Agarwal, A.; Misra, G. Review and Performance Analysis on Wireless Smart Home and Home Automation using IoT. In Proceedings of the 2019 Third International conference on I-SMAC (IoT in Social, Mobile, Analytics and Cloud) (I-SMAC), Palladam, India, 12–14 December 2019; pp. 629–633. [[CrossRef](#)]
37. Tayef, S.H.; Rahman, M.M.; Sakib, M.A.B. Design and Implementation of IoT based Smart Home Automation System. In Proceedings of the 2021 24th International Conference on Computer and Information Technology (ICCIT), Dhaka, Bangladesh, 18–20 December 2021; pp. 1–5. [[CrossRef](#)]
38. Alsoub, N.; Thirunilath, N.M.; Ali, I. Smart Home Automation IoT System for Disabled and Elderly. In Proceedings of the 2022 IEEE International IOT, Electronics and Mechatronics Conference (IEMTRONICS), Toronto, ON, Canada, 1–4 June 2022; pp. 1–5. [[CrossRef](#)]
39. Drzewiecki, M.; Guziński, J. Design of autonomous IoT node powered by a perovskite-wased wave energy converter. *Pol. Marit. Res.* **2023**, *3*, 142–152. [[CrossRef](#)]
40. Mpicosys Low Power Innovators Invent, Design & Produce for You. Available online: <https://www.mpicosys.com/> (accessed on 11 February 2023).
41. Woo, M.S.; Baek, K.H.; Kim, J.H.; Song, D.; Sung, T.H. Relationship between current and impedance in piezoelectric energy harvesting system for water waves. *J. Electroceram.* **2015**, *34*, 180–184. [[CrossRef](#)]
42. Urone, P.P.; Hinrichs, R. College Physics. Chapter 19.7 Energy Stored in Capacitors. OpenStax. 2012. Available online: <https://openstax.org/books/college-physics/pages/19-7-energy-stored-in-capacitors> (accessed on 12 November 2023).
43. Urone, P.P.; Hinrichs, R. College Physics, Chapter 20.4 Electric Power and Energy. OpenStax. 2012. Available online: <https://openstax.org/books/college-physics/pages/20-4-electric-power-and-energy> (accessed on 12 November 2023).

**Disclaimer/Publisher’s Note:** The statements, opinions and data contained in all publications are solely those of the individual author(s) and contributor(s) and not of MDPI and/or the editor(s). MDPI and/or the editor(s) disclaim responsibility for any injury to people or property resulting from any ideas, methods, instructions or products referred to in the content.

